

Impurities and Screening Effect in Hydrogen and Helium Discharges of Large Helical Device

S.Morita, M.Goto, T.Morisaki, S.Inagaki, M.Emoto, H.Funaba, K.Ida, H.Idei, S.Kado, O.Kaneko, K.Kawahata, T.Kobuchi, A.Komori, S.Kubo, R.Kumazawa, S.Masuzaki, T.Minami, J.Miyazawa, O.Motojima, S.Murakami, S.Muto, T.Mutoh, Y.Nagayama, Y.Nakamura, H.Nakanisi, K.Narihara, K.Nishimura, N.Noda, S.Ohdachi, N.Ohyabu, Y.Oka, M.Osakabe, T.Ozaki, B.J.Peterson, A.Sagara, S.Sakakibara, R.Sakamoto, H.Sasao, K.Sato, M.Sato, T.Seki, T.Shimozuma, Y.Shirai, M.Shoji, T.Sugie¹, H.Suzuki, Y.Takeiri, K.Tanaka, K.Toi, T.Tokuzawa, K.Tsumori, K.Tsuzuki, B.N.Wan², K.Y.Watanabe, T.Watari, I.Yamada, H.Yamada, S.Yamaguchi

National Institute for Fusion Science, Toki 509-5292, Gifu, Japan

¹*JAERI, Naka 311-0193, Ibaraki, Japan*

²*Institute of Plasma Physics, Academia Sinica, 230031, Hefei, Anhui, China*

1. Introduction

LHD ($R/a=3.75/0.6\text{m}$, $l/m=2/10$, $B_t=3\text{T}$, $V_p=30\text{m}^3$) started an ECH experiment on March 1998. After several kinds of wall conditionings such as baking (100°C), ECR and glow discharge cleanings and Ti gettering the plasma performance was gradually improved. Experiments finished on December 1998 with successful results¹ (84GHz ECH, 100keV NBI, 26MHz ICRF, $m/n=1/1$ LID) including a first trial of steady state operations (<22sec for NBI, a few minutes for ECH), whereas any modification on the vacuum vessel (SS316), especially at the divertor section, was not made. In this paper we describe results on impurities, Z_{eff} and screening effect in relation to an improvement of the plasma performance obtained through the 1st and 2nd experimental campaigns.

2. Impurities and Z_{eff}

LHD was operated with hydrogen and helium discharges. In most of the hydrogen discharges a density reduction appeared and disturbed a smooth density rise. As a result, the density was limited up to $3 \times 10^{13} \text{cm}^{-3}$ except for a few shots at inwardly shifted magnetic configuration ($R_{\text{ax}}=3.6$) in high-field operation (2.5T). The discharge was frequently collapsed by a strong gas puffing, when a higher density operation was tried. According to the strong H_2 gas puffing, $\text{H}\alpha$ emissions from an x-point increased with a density rise at ergodic layer outside LCFS, although a flat $\text{H}\alpha$ profile was generally observed. After switching off the gas puffing, metallic impurities come into the plasma because of the rapid edge temperature rise. On the contrary the helium discharge showed a smooth density rise during the gas puffing phase in most of the shots. After turning off the gas puffing, however, the density generally does not drop keeping the same density level until the end of the discharge. It was really difficult to control and adjust an expected density level. The radiation loss also became severe and the radiation collapse happened during discharges², especially in the low magnetic field case ($B_t=1.5\text{T}$). In helium discharges the main radiation originates in iron (0.1-0.2% of n_e) coming from the vacuum wall at divertor section and the collapse occurs from the plasma center in a few cases, although the collapse is initiated from the plasma edge in hydrogen case. The oxygen and carbon concentrations were roughly 1% of n_e and the radiation from them was located in the ergodic layer outside the LCFS.

Figure 1 shows toroidal distributions of $\text{H}\alpha$ and CIII emissions indicating toroidal uniformity of each element, though carbon armor tiles are set (#2 and #9 toroidal sections) for protection of vacuum vessel from negative high-energy NBIs. Any serious nonuniformity

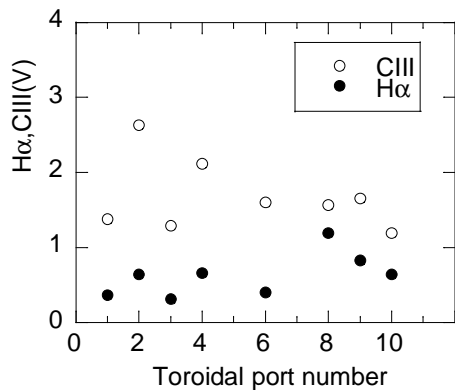


Fig.1 Toroidal distribution of H α and CIII.

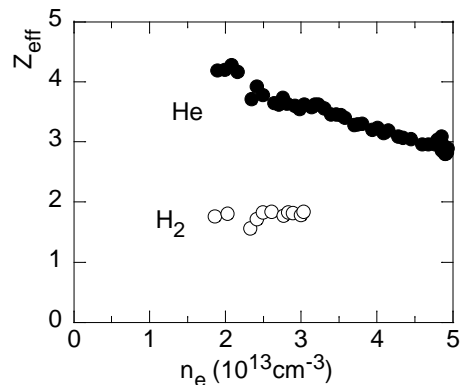


Fig.2 Z_{eff} as a function of n_e .

was not observed even in the low-density NBI operation less than $1 \times 10^{13} \text{cm}^{-3}$. The values of Z_{eff} are measured from visible bremsstrahlung as a typical monitor of impurity concentration (see Fig.2). The values are typically around 2 for H_2 discharges and 3-4 for He discharges except for unconditioned shots, although the NBI power is still low ($< 3 \text{MW}$) in comparison with the plasma volume. The Z_{eff} profiles are also measured through an optical fiber array. A preliminary result is shown in Fig.3. The emission from the plasma edge includes visible line emissions. After the Abel inversion the distribution of the bremsstrahlung also had a sharp peak at the edge region. Then, the large value of the Z_{eff} , especially at $\rho = 1$, does not indicate the true Z_{eff} value. The Abel-inverted density profile used in the $Z_{text{eff}}$ analysis is also shown in Fig.4. At present the obtained Z_{eff} profile is seemed to be much similar to the density profile. Most of the Z_{eff} profiles are flat and it was roughly the same as the density profile, although the data which are applicable to the analysis are limited. No peaking profiles are observed until now.

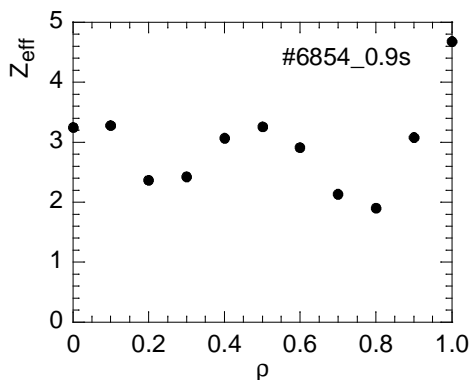


Fig.3 Z_{eff} profile of He discharge.

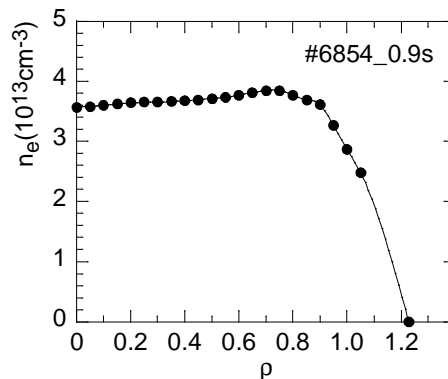


Fig.4 Density profile as a function of ρ

3. Screening Effect

In helical research it is important to study the role of the ergodic layer surrounding LCFS. Especially, LHD is a first helical machine having a divertor configuration. Physical relations among divertor, ergodic layer and core plasmas have to be investigated. The density reduction generally appears in LHD and is observed mainly for H_2 discharges, as mentioned above. We studied the role of the edge plasma produced in the ergodic layer in relation to the density reduction at the core plasma.

Figure 5 shows a typical NBI discharge ($B_t = 1.5 \text{T}$, $R_{\text{ax}} = 3.75 \text{m}$, $P_{\text{NBI}} = 1 \text{MW}$). The plasma density suddenly reduces at $t = 0.68 \text{s}$, whereas the gas puffing is enough carried out. After the reduction of the density the gas puffing rate is reduced for avoiding the plasma collapse. The $\text{H}\alpha$ intensity does not change until the end of discharge. The edge temperature at the ergodic layer is obtained from YAG Thomson scattering system (see Fig.6), which measures $T_e(R)$ along the major radius direction at a horizontally elongated toroidal

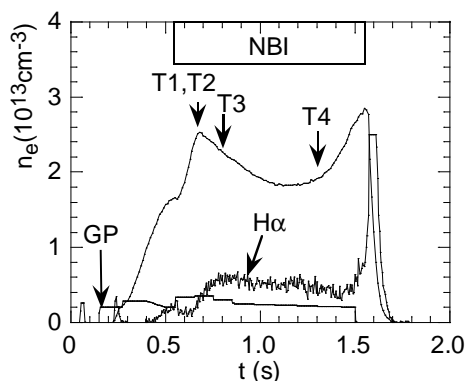


Fig.5 Time behavior of n_e .

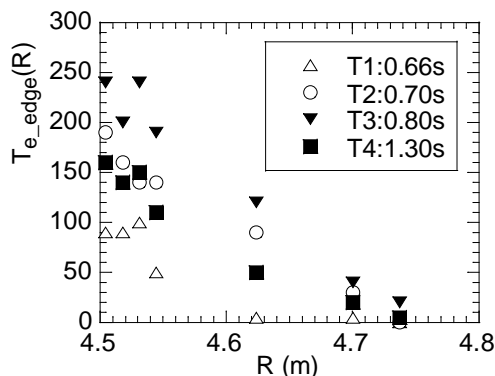


Fig.6 Time behaviors of $T_e(r)$ at ergodic layer

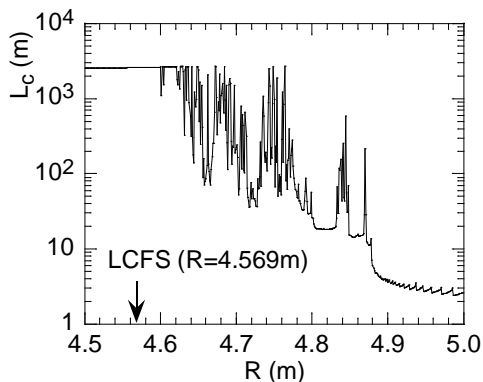


Fig.7 Connection length at ergodic region.

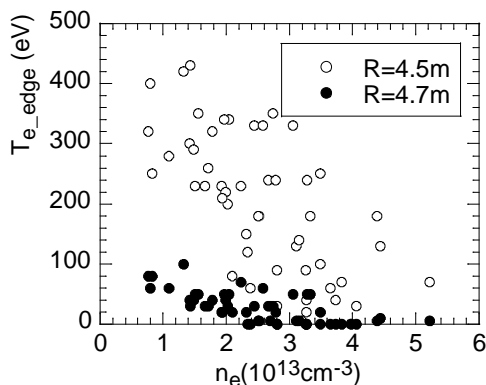


Fig.8 Edge T_e at ergodic layer against n_e .

section. The position of the LCFS is $R=4.569\text{m}$ at vacuum pressure (see Fig.7). It can be seen that the plasma expands rapidly toward the ergodic layer and it continues until the density reduction happens. In this shot the plasma radius is maintained inside $R=4.75\text{m}$ in which the connection length is at least longer than 100m . After the plasma front reaches this

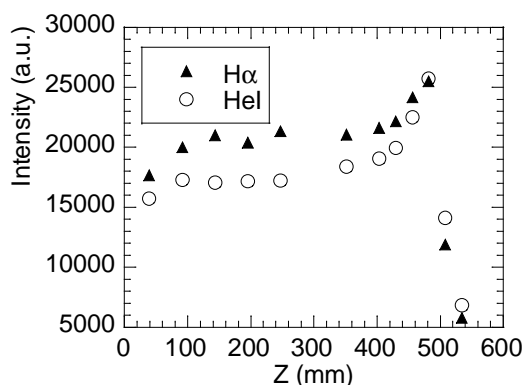


Fig.9 Radial profiles of $H\alpha$ and HeI

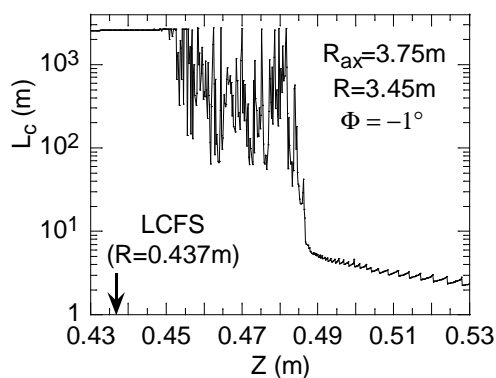


Fig.10 Connection length at $H\alpha$ position.

region ($R=4.75\text{m}$) the density drops immediately. At the same time it is measured from the electric static probe that the particle flux coming to the divertor leg suddenly increases³. When such an edge temperature is kept, the density increases no more. In this shot the density goes up after 1.3s again. At the end of the discharge ($t=1.3\text{s}$) the edge temperature decreases gradually because of the buildup of impurities. The plasma radius begins to shrink and the neutral source closes to the LCFS. The divertor particle flux decreases and the density increases again. The relation between the edge temperature and line-averaged density is examined as shown in Fig.8. The data include variations in P_{NBI} and B_t . We can understand that such a high-temperature at the ergodic region is realized only in the density

range less than $2 \times 10^{13} \text{cm}^{-3}$. In other words, the discharges in high-density range, mainly obtained for He discharges, shrink near the LCFS.

H α radial profiles are observed with a combination of optical fibers, visible spectrometer and CCD detector. A typical result is shown in Fig.9. The data are obtained from a parallel fiber array at upper side of a horizontally elongated plasma position. The value of Z means the vertical direction. The peak position of the profile locates around Z=480mm. The connection length at the line-of-sight of the optical fiber is shown in Fig.10. We can understand the particle source exists in the ergodic layer outside the LCFS shortly connected with the divertor leg.

4. Limiter Experiment

The screening effect as mentioned above may become a serious problem in large helical machines. The question is how we can get a smooth density rise keeping a high-temperature divertor condition. Then, we carried out a limiter experiment to cut the ergodic layer plasma. The guard limiter for protection of a movable ICRF antenna was used for the purpose. The limiter is installed from the outboard (high-field) side at a vertically elongated position. The results are shown in Fig.11. Before insertion of the limiter ($R_{\text{lim}}=4.22\text{m}$) the

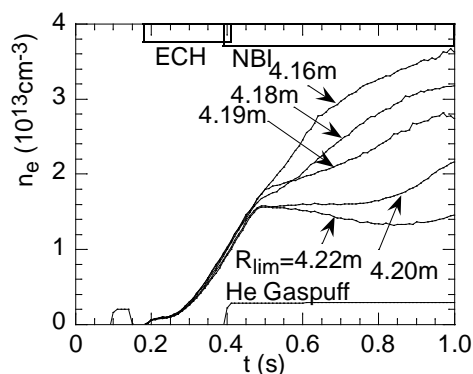


Fig.11 Time behaviors of n_e as a parameter of limiter positions.

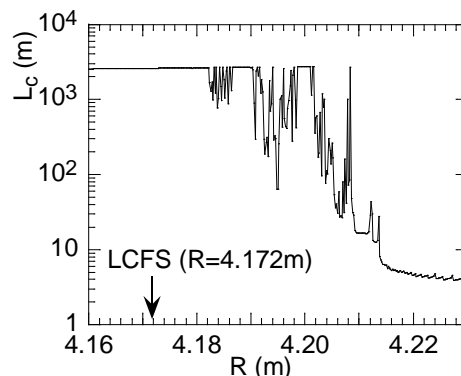


Fig.12 Connection length L_c and LCFS at outboard side of vertically elongated position ($R_{\text{ax}}=3.75\text{m}$).

density reduction appears at $t=0.47\text{s}$. According to the movement of the limiter head position the density behavior largely changes. Here, it is pointed out from the data of the Thomson scattering and soft x-ray array that the boundary of the plasma is clearly defined by the limiter position. In order to get a smooth density rise we can see the limiter has to be inserted at least at $R=4.19\text{m}$. It should be noticed that the position of the $R=4.19\text{m}$ has a long connection length more than 1km as shown in Fig.12. When the particle source is moved to those regions, the ionized particles will be smoothly linked to the LCFS.

5. Remarks for Future Experiments

The metallic impurities become dominant for helium and hydrogen discharges, especially after turning off gas puffing, although they may be also screened by the ergodic layer. The carbon tiles were installed as a divertor plate for next (3rd) experimental campaign. The metallic impurities will be surely reduced. The creation of magnetic islands and the use of LID (local island divertor) will be one of candidates to delete the inefficient fuelling problem in relevant to the screening effect due to the ergodic layer plasma. The pump limiter for the LID will be installed on LHD in near future. The pellet injection for fuelling is also started. The increase of NBI power up to 8MW is now being carried out. They will possibly reduce the present experimental difficulty on the impurity and fuelling problems.

References

1. O.Motojima, H.Yamada, A.Komori, et al., Phys. Plasma 6, 1843 (1999).
2. S.Masuzaki, et al., this conference.
3. B.J.Peterson, et al., this conference.